



ELSEVIER

Available online at www.sciencedirect.com

SCIENCE @ DIRECT®

Journal of Constructional Steel Research 61 (2005) 1595–1612

JOURNAL OF
CONSTRUCTIONAL
STEEL RESEARCH

www.elsevier.com/locate/jcsr

Development of moment–rotation model equations for flush end-plate connections

Ali Abolmaali^{a,*}, John H. Matthys^a, Mohammed Farooqi^b,
Yeol Choi^c

^a*Department of Civil and Environmental Engineering, University of Texas at Arlington, Arlington,
TX 76019, United States*

^b*Jerrald W. Kunkel Consulting Engineers, Arlington, TX 76019, United States*

^c*Kyungpook National University, Taegu 702-701, Republic of Korea*

Received 6 January 2005; accepted 3 May 2005

Abstract

This paper presents the development of Ramberg–Osgood and Three-Parameter Power model prediction equations for the moment–rotation (M – θ) behavior of flush end-plate connections with one row of bolts below tension and compression flanges. A finite element model (FEM) of the connection region along with the connected beam and column is developed for load deformation analyses, which included material, geometric, and contact nonlinearities. The FEM model was verified with test results conducted and reported for flush end-plate connections in the literature during the 1980s. A matrix of test cases was obtained by varying the geometric variables of flush end-plate connections within their practical ranges. The connection M – θ data for these test cases were obtained by FEM analyses, which were then curve fitted to Ramberg–Osgood and Three-Parameter Power model equations to obtain parameters defining these equations. Finally, prediction equations were developed for parameters of the model equations as functions of geometric variables of the flush end-plate connections.

© 2005 Elsevier Ltd. All rights reserved.

Keywords: Steel connection; Moment–rotation equations; Ramberg–Osgood; Three-parameter power model; Connection stiffness; Connection strength

* Corresponding address: Department of Civil and Environmental Engineering, University of Texas at Arlington, PO Box 19308, Arlington, TX 76019, United States.

E-mail address: abolmaali@ce.uta.edu (A. Abolmaali).

1. Introduction

Moment rotation ($M-\theta$) characteristics of bolted or bolted/welded steel connections are indicative of the connection's stiffness, strength, and ductility. Experimentally obtained $M-\theta$ behavior is entirely dependent upon and highly sensitive to the connection's geometric variables (i.e., plate/angle thickness, bolt diameter, bolt pitch, bolt gauge, etc).

Studies relating to rotational stiffness of beam-to-column connections historically go back to early 1900. Wilson and Moore [1] conducted several tests to establish the relationship between moments and relative rotations of beam-column connections. Prior to 1950, riveted connections were tested by Rathbun [2]. Next, the use of high-strength bolts as structural fasteners was tested by Bell et al. [3]. Douty and McGuire [4] reported the importance of end-plate thickness on the strength of connections based on a limited test series of five flush end-plate connections.

Subsequently, the behavior of header plate connections was experimentally investigated by Sommer [5]. Since the late 1960s, flush end-plate and extended end-plate connections for use as moment connections have been investigated extensively by Ostrander [6] and Johnstone and Walpole [7], respectively. Srouji et al. [8] conducted several experimental testing and yield line analyses on flush end-plate connections with one and two rows of bolts below the tension flange. In this study yield line analysis closely predicted the strength of the connection. Azizinamini and Radzimirski [9] performed 18 static tests on top and seat flange angles and double web angle connections. It was shown that the geometric parameters significantly affected the $M-\theta$ performance.

Several researchers have proposed experimentally based theoretical and mathematical models to represent the $M-\theta$ behavior of the tested connections. Many research projects have been carried out in the past few decades to classify the connection types and to develop the mathematical model for connection stiffness. Frye and Morris [10] collected 145 test data and classified seven types of connection tests ranging from the weakest single web angle connection to the stiffest T-stub connection. They modeled the $M-\theta$ relationship by a polynomial function which was previously adopted by Sommer [5]. Ang and Morris [11] collected 32 $M-\theta$ results from experiments, conducted from 1934 to 1976, and grouped into five types, namely the single web angle, the double web angle, the header plate, the top and seat angle and the strap angle connections. The Ramberg-Osgood function presented by Ramberg and Osgood [12] was used to represent the standardized moment-rotation relationship for the five commonly used connection types. Packer and Morris [13], Zoetemeijer [14], and Phillips and Packer [15] utilized straight and curved yield line mechanisms to predict end-plate moment capacity in flush end-plate connections.

Bijlaard and Zoetemeijer [16] conducted studies on semi-rigid frames and concluded that a complete classification of semi-rigid connections must take into account the ratio between the connection stiffness and the beam stiffness. Bjorhovde et al. [17] concluded that the framework and its members and connections exhibit semi-rigid nonlinear response characteristics. They also reported that connection flexibility can produce significantly larger second-order $P-\Delta$ effects in the structure that must be accounted for in the design. Bjorhovde et al. [18] developed a scheme to classify connections using test and theoretical data. This scheme uses stiffness, ultimate strength, and ductility requirements, which is applicable to old and new connections. Barakat and Chen [19] incorporated connection

stiffness considerations into the established AISC-LRFD design approach using two proposed connection models. The first model uses a modified initial stiffness representation and the second model is determined by the beam-line method. Xu et al. [20] used empirical data to represent the stiffness of partially restrained (PR) connections. However, the resulting moment–rotation curves offered little practical value to the designer, since connection behavior (i.e. strength and stiffness) is highly dependent on the connecting members.

Yee and Melchers [21] developed mathematical equations for end-plate moment connections using experimentally obtained data. Kishi and Chen [22,23] extended the collection of the steel connection $M-\theta$ data to include results from 300+ tests, classified into seven connection types. They introduced several $M-\theta$ models, of which the Three-Parameter Power model gained most attention. Stark and Bijlaard [24] introduced simplified methods to develop bilinear models to represent typical nonlinear $M-\theta$ curves.

The aforementioned studies and others used the time consuming experimental data to develop $M-\theta$ equations, which limits the variation of connection geometry in the test matrix. While some researchers such as Krishnamurthy [25], Ghassemieh et al. [26] and Bahaari and Sherbourne [27,28] developed detailed finite element method (FEM) models for large capacity extended end-plate connections and compared their analysis results with those of experiments, the development of FEM-based model equations was outside the scope of their studies. Summer et al. [29] conducted a series tests on four bolt extended unstiffened and the eight bolt extended stiffened end-plate connections along with a validation study utilizing the finite element method. This study showed that extended moment end-plate connections can be designed to provide ductility in seismic force resisting moment frames.

Thus, this paper presents the development of two types of $M-\theta$ model equations for flush-end plate connections with one bolt row below the tension flange (Fig. 1) based on material, geometric, and contact nonlinear FEM analyses of connection region. The accuracy of the FEM and its results are verified by using experimentally obtained $M-\theta$ curves by Srouji et al. [8]. A test matrix with 34 test specimens is introduced by varying the geometric variables of the flush end-plate connection within its practical range from low to intermediate to high values. These test cases were analyzed using the developed FEM model and the resulting $M-\theta$ data were curve fitted to Ramberg–Osgood [12] and Three-Parameter Power model [22,23] equations, and regression equations were developed for the parameters defining these model equations. Finally, predicted $M-\theta$ curves using Ramberg–Osgood and Three-Parameter equations were compared with those obtained from experimental FEM analyses.

2. Finite element model

A three-dimensional nonlinear FEM connection model, for the flush end-plate connections of the type shown in Fig. 2, is generated using the finite element analysis software package, ANSYS. Since a plane of symmetry exists along a section through the beam web, one-half of the connection region including column and beam was modeled.

In the three-dimensional model, 8-noded solid isoparametric elements were used to model the beam, column, end-plate and bolt. The complex interaction between the surfaces

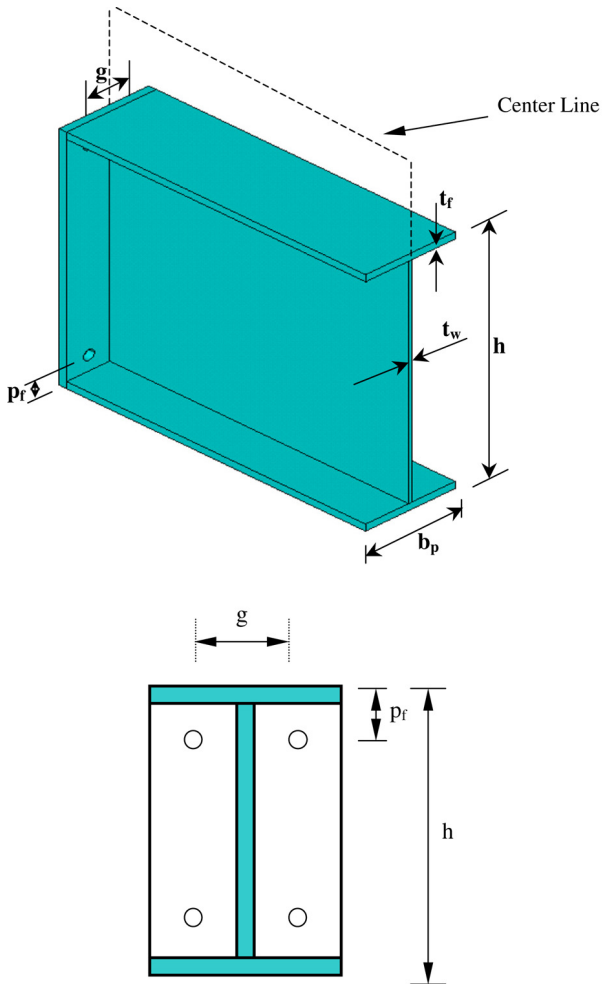


Fig. 1. Configuration of flush end-plate connection.

of the end-plate and column flange, bolt head/nut and end-plate, and bolt shank and end-plate were modeled with the node-to-node contact and target elements. The welds were modeled with three-dimensional tetrahedral elements.

The end-plate and bolt material behavior was described by bilinear stress–strain curves as shown in Fig. 3 with initial slope of the curve being taken as the elastic modulus, E , of the material. After several trials to best calibrate the FEM model with the experimental results obtained by Srouji et al. [8], the post-yield stiffness identified as the tangent modulus, E_t , was taken as 10% of the initial stiffness ($E_t = 0.1E$). Plasticity-based isotropic hardening, which uses the von Mises yield criteria coupled with an isotropic work hardening assumption, was used to obtain the response of the connection in the inelastic region.

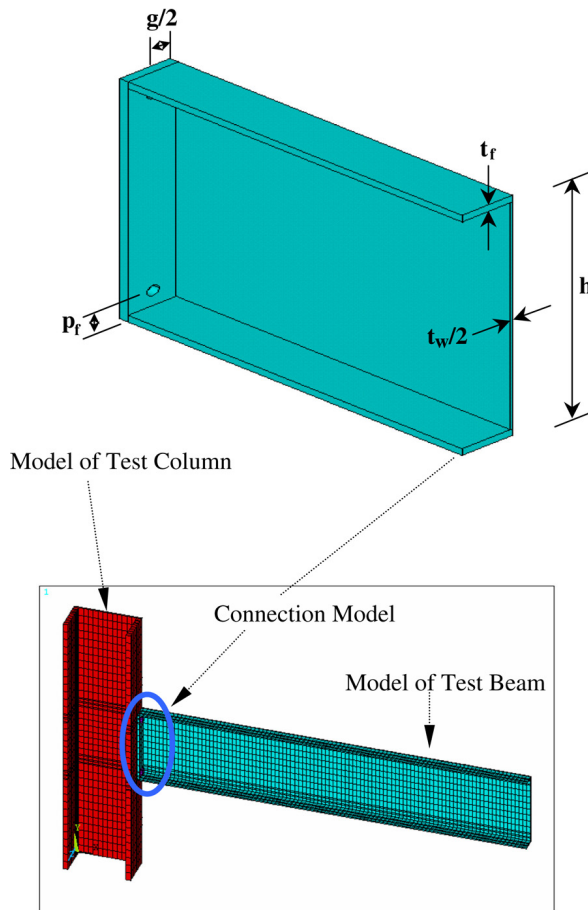


Fig. 2. FEM model of the flush end-plate connection.

In the early finite element studies of bolted connections such as those by Choi and Chung [30], pretension effects in the bolts caused by the tightening of each bolt were simulated by applying compressive forces equivalent to proof load (70% of bolt's ultimate tensile strength) to the end-plate at the location of the bolt head and nut. This would introduce difficulties in monitoring the variation of the bolt force during the analysis. Thus, ANSYS's bolt pretension element was used, which is a three-dimensional line element that acts as a connecting element to connect the two imaginary parts of the bolt shank. The pretension element, as shown in Fig. 4, contains nodes "I" and "J" located at an arbitrary section through the bolt shank length which are connected with a link element. The aforementioned section is selected arbitrarily in order to comply with different mesh configurations. Node K is the pretension node with one degree of freedom, u_x , with the actual line of action in the pretension load direction. The underlying bolt elements can be solid, shells, or beam elements, of any order of polynomial. When the pretension is applied on

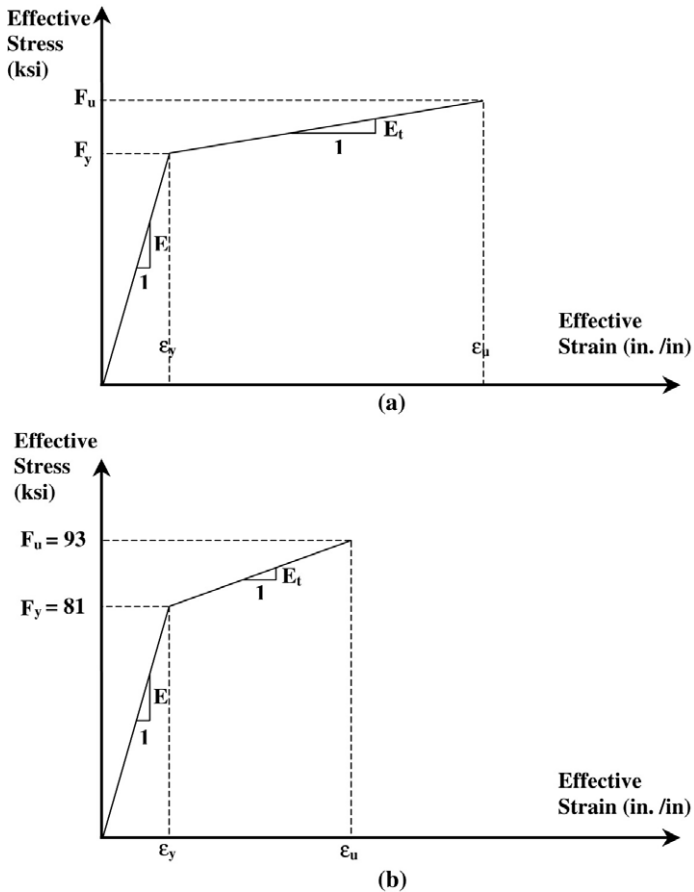


Fig. 3. Idealized material behavior used in the FEM analysis for: (a) end-plate, beam, and column materials and (b) A-325 high strength bolts.

the node K, the link element joining nodes I and J will be in tension; this in turn pulls the two imaginary sections of the bolt towards each other to compress the connecting surfaces.

During the pretensioning of a physical bolt, turning of the nut reduces the unstretched grip length of the bolt, thereby inducing pretension. When the desired pretension is achieved and the wrench is removed, the new unstretched grip length becomes locked. The pretension element used applies the same procedure during the loading in the same sequence. First, the specified pretension load is applied incrementally to capture contact nonlinearity, and possible nonlinearities induced by material yielding. For example, tightening a 3/4 in bolt with 28 k pretension load may yield a 1/4 in end-plate at the pretensioning stage. At this point in the analysis, the pretension section displacement is locked for the pretensioned bolt. Once all bolts are pretensioned and locked, external load is applied incrementally to capture nonlinearities due to material, geometric, and contact. Since the monotonic convergence of nonlinear problems by the finite element method in

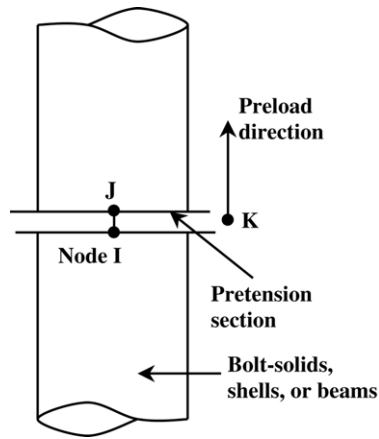


Fig. 4. ANSYS's pretension element.

general is problem dependent and not guaranteed, improved convergence was obtained with an energy-based method.

3. Comparison with experimental test results

The experimental data obtained by Srouji et al. [8] were used to validate the FEM model developed in this research. The details of the test specimens are presented in Table 1 and are identified by FI- d_b - t_p - h indicating one bolt row flush end-plate connection (FI), bolt diameter (d_b), end-plate thickness (t_p), and beam depth (h), respectively. The comparison of typical three-dimensional finite element and experimental results for applied moment versus rotation are depicted in Figs. 5 through 7. In these figures the M - θ plots obtained from FEM analyses are those of converged solutions with respect to both mesh refinement and load steps.

4. Selection of test cases

To conduct the parametric study, it was decided to vary the geometric variables within the practical ranges of flush end-plate connections based on usual detailing practices given in Srouji [8] as tabulated in Table 2. Based on the ranges of variables defined in this table, the following procedure was adopted to select the beam dimensions:

1. Four values of beam depth, h , were selected based on maximum and minimum value of h given in Table 2. The four values selected were 10, 16, 24 and 30 in.

2. For each value of beam depth, four values of beam flange width, b_f ($= b_p$, end-plate width), were considered as follows: $h/6$, $h/5$, $h/4$ and $h/3$. However, a limitation was put on b_f such that $b_f \geq 2$ in.

3. For each value of beam flange width, four values of beam flange thickness, t_f , were considered as follows: $b_f/35$, $b_f/26$, $b_f/16$ and $b_f/6$. A limitation was put on t_f such that $t_f \geq 0.1$ in.

Table 1
Geometric variables of the tests conducted by Srouji [8]

Test no.	Test designation	Bolt diameter d_b	End-plate thickness t_p	Beam depth h	Flange width b_f	Pitch p_f	Gage g	Yield stress
1	Fl-3/4-1/2-16	3/4 (in.)	1/2 (in.)	16 (in.)	6 (in.)	1 1/2 (in.)	3 1/2 (in.)	55.48 (ksi)
	Fl-19-13-406	19 (mm)	13 (mm)	406 (mm)	150 (mm)	38 (mm)	90 (mm)	382 (MPa)
2	Fl-3/4-3/8-16	3/4 (in.)	3/8 (in.)	16 (in.)	6 (in.)	1 1/2 (in.)	3 1/2 (in.)	59.45 (ksi)
	Fl-19-10-406	19 (mm)	10 (mm)	406 (mm)	150 (mm)	38 (mm)	90 (mm)	410 (MPa)
3	Fl-5/8-1/2-16	5/8 (in.)	1/2 (in.)	16 (in.)	6 (in.)	1 7/8 (in.)	3 3/4 (in.)	53.98 (ksi)
	Fl-16-13-406	16 (mm)	13 (mm)	406 (mm)	150 (mm)	48 (mm)	95 (mm)	372 (MPa)
4	Fl-5/8-3/8-16	5/8 (in.)	3/8 (in.)	16 (in.)	6 (in.)	1 3/8 (in.)	2 3/4 (in.)	56.95 (ksi)
	Fl-16-10-406	16 (mm)	10 (mm)	406 (mm)	150 (mm)	35 (mm)	70 (mm)	393 (MPa)
5	Fl-5/8-3/8-10	5/8 (in.)	3/8 (in.)	10 (in.)	5 (in.)	1 1/4 (in.)	2 1/4 (in.)	51.90 (ksi)
	Fl-16-10-250	16 (mm)	10 (mm)	250 (mm)	125 (mm)	32 (mm)	57 (mm)	356 (MPa)
6	Fl-5/8-1/2-10	5/8 (in.)	1/2 (in.)	10 (in.)	5 (in.)	1 1/2 (in.)	3 (in.)	55.80 (ksi)
	Fl-16-13-250	16 (mm)	13 (mm)	250 (mm)	125 (mm)	38 (mm)	75 (mm)	385 (MPa)
7	Fl-3/4-1/2-24A	3/4 (in.)	1/2 (in.)	24 (in.)	6 (in.)	1 3/4 (in.)	3 1/4 (in.)	57.53 (ksi)
	Fl-19-13-610A mm	19 (mm)	13 (mm)	610 (mm)	150 (mm)	45 (mm)	83 (mm)	397 (MPa)
8	Fl-3/4-1/2-24B in.	3/4 (in.)	1/2 (in.)	24 (in.)	6 (in.)	1 3/8 (in.)	2 3/4 (in.)	57.53 (ksi)
	Fl-19-13-610B mm	19 (mm)	13 (mm)	610 (mm)	150 (mm)	35 (mm)	70 (mm)	397 (MPa)

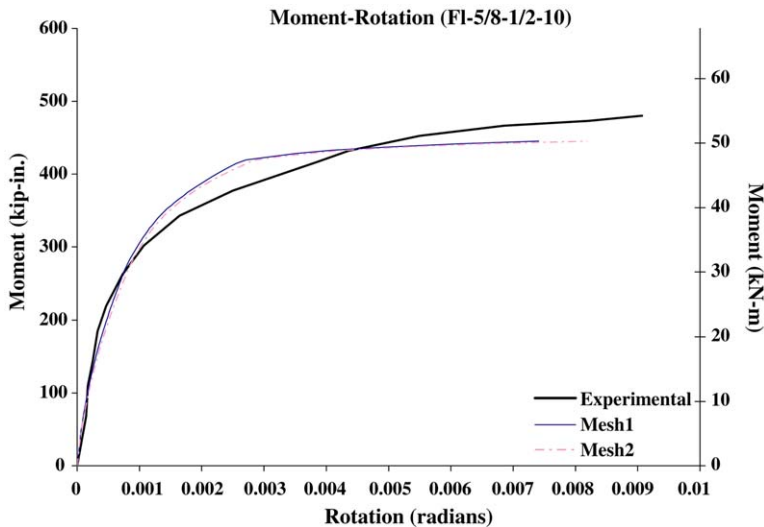


Fig. 5. Comparison of converged FEM obtained moment–rotation plot with experimental results obtained by Srouji et al. [8] for Fl-5/8-1/2-10.

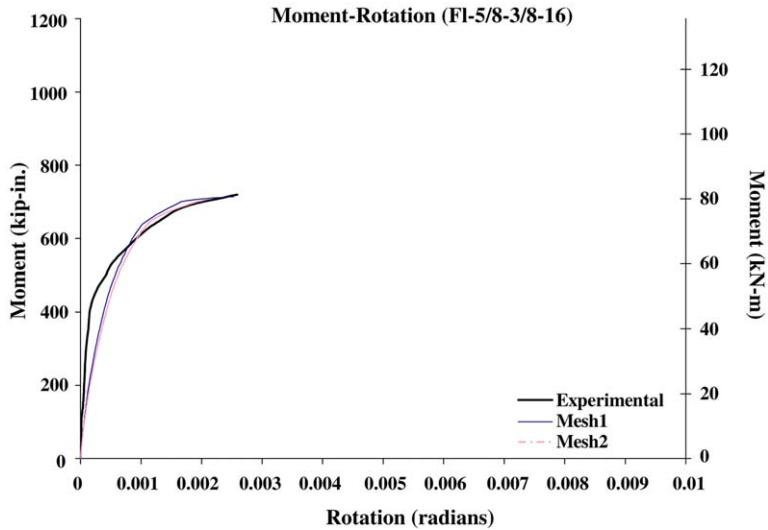


Fig. 6. Comparison of converged FEM obtained moment–rotation plot with experimental results obtained by Srouji et al. [8] for FI-5/8-3/8-16.

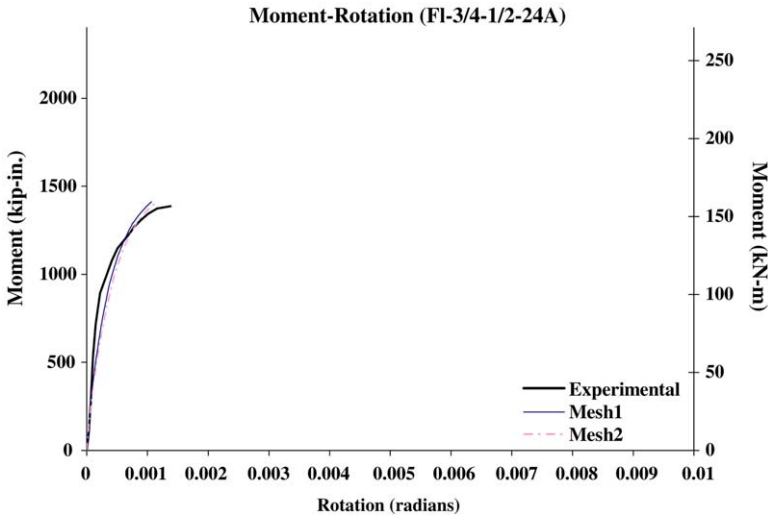


Fig. 7. Comparison of converged FEM obtained moment–rotation plot with experimental results obtained by Srouji et al. [8] for FI-5/8-3/8-16.

4. For each value of beam depth, four values of beam web thickness, t_w , were considered as follows: $h/160$, $h/133$, $h/107$ and $h/80$. A limitation was put on t_w such that $t_w \geq 0.1$ in.

Based on the combination of the aforementioned variables by keeping each variable at its intermediate value one at a time while varying other variables from low to intermediate

Table 2
Practical ranges for geometric parameters Srouji [8]

Parameter	Low	Intermediate	High
g	2 1/4 (in.) 57 (mm)	2 3/4 (in.) 70 (mm)	3 1/2 (in.) 83 (mm)
d_b	5/8 (in.) 16 (mm)	3/4 (in.) 19 (mm)	1 (in.) 25 (mm)
p_f	1 1/8 (in.) 29 (mm)	1 3/4 (in.) 44 (mm)	2 1/2 (in.) 63 (mm)
b_p	5 (in.) 127 (mm)	7 (in.) 178 (mm)	10 (in.) 254 (mm)
t_p	5/16 (in.) 7.94 (mm)	1/2 (in.) 12.70 (mm)	3/4 (in.) 19 (mm)
t_f	0.18 (in.) 4.60 (mm)	0.375 (in.) 9.50 (mm)	0.50 (in.) 12.70 (mm)
t_w	0.10 (in.) 2.54 (mm)	0.1875 (in.) 4.76 (mm)	0.25 (in.) 6.35 (mm)
h	10 (in.) 254 (mm)	24 (in.) 609 (mm)	30 (in.) 762 (mm)

to high, 256 of the different beam cross-sections obtained, which fell within the range of the variables given in Table 2. From the 256 cases, the 34 most proportional test cases were selected for the regression analysis.

5. Development of $M-\theta$ equation

The finite element $M-\theta$ results obtained from the selected 34 cases in the preceding section were curve fitted to the Ramberg–Osgood and Three-Parameter Power models. First, brief backgrounds on both model equations are presented.

The Ramberg–Osgood model was originally proposed by Ramberg and Osgood [12] and later standardized by Ang and Morris [11]. The general form of the moment–rotation curve of the model is:

$$\frac{\theta}{\theta_y} = \frac{|M|}{M_y} \left[1 + \left(\frac{|M|}{M_y} \right)^{\xi-1} \right] \quad (1)$$

where M_y and θ_y are characteristics moment and rotation, respectively, which define the position of the intersection point P in Fig. 8 through which a family of Ramberg–Osgood curves passes, and the shape of which is influenced by the shape parameter, ξ . This figure shows that, as the shape parameter increases, the $M-\theta$ curve becomes more flexible. The Ramberg–Osgood model requires only three parameters, and experimental data can be fitted to the model.

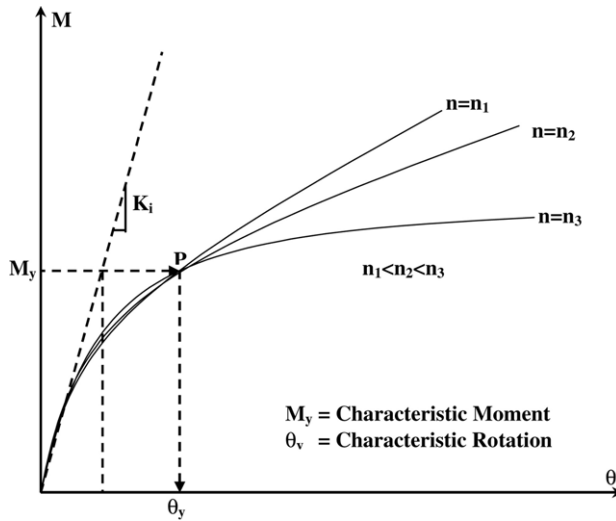


Fig. 8. Ramberg–Osgood model.

The Three-Parameter Power model was originally proposed by Richard and Abbott [31] and Chen and Kishi [23,32] to predict the moment–rotation ($M-\theta$) characteristics of semi-rigid connections. There are three independent parameters that define this model equation, which are: initial stiffness, K_i , ultimate moment, M_u , and rigidity parameter, ζ . This equation is described by:

$$M = \frac{K_i \theta}{[1 + (\theta/\theta_0)^\zeta]^{\frac{1}{\zeta}}} \tag{2}$$

where

- M_u = ultimate moment capacity
- ζ = rigidity parameter
- K_i = initial connection stiffness
- θ_0 = reference plastic rotation defined by:

$$\theta_0 = M_u / K_i. \tag{3}$$

Fig. 9 shows the schematic of the Three-Parameter Power model with different values of rigidity parameter, ζ , which defines a more flexible model as ζ increases.

In this study, the 34 test cases selected were analyzed using the FEM connection model developed in Section 2. The $M-\theta$ data points obtained from these analyses were curve fitted to Eqs. (1) and (2) by minimizing their error-square to obtain model parameters M_y , θ_y , and ξ and M_u , θ_0 , and ζ for the Ramberg–Osgood (RO) and Three-Parameter Power (TPP) equations, respectively. Consequently, regression equations were developed for the aforementioned parameters of each equation in terms of geometric variables of the connection region. In the development of the prediction equations, the *independent variables* (connection geometric variables) are defined as:

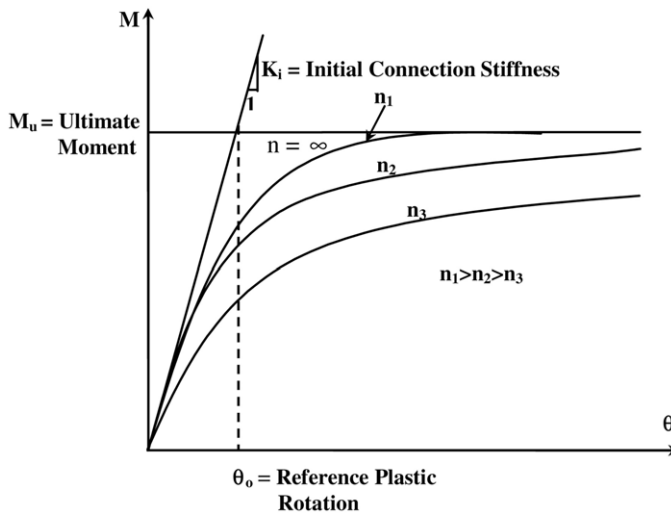


Fig. 9. Three-Parameter Power model.

- g = the gage distance
- d_b = the nominal bolt diameter
- p_f = the bolt pitch
- b_p = the width of end-plate
- t_p = the thickness of end-plate
- t_f = the beam flange thickness
- t_w = the beam web thickness
- h = the beam depth
- F_y = material yield stress.

The *dependent variables* for each of the model equations are defined as follows:

For the Ramberg–Osgood model:

M_y = Characteristic moment

θ_y = Characteristic rotation

ξ = Shape parameter

For the Three-Parameter Power model:

M_u = Ultimate moment

θ_0 = Reference plastic rotation as defined by Eq. (3)

ζ = Rigidity parameter.

From regression analyses, Eqs. (4)–(6) predict independent parameters of the Ramberg–Osgood equation for characteristic moment, characteristic rotation, and shape parameter, respectively. Similarly, Eqs. (7)–(9) represent independent parameters of the Three-Parameter Power equation for ultimate moment, reference plastic rotation, and rigidity parameter, respectively. Sensitivity and error band analyses were conducted to validate the behavior of each equation to the variation of independent variables and the

error associated with each equation, respectively. The details of these studies are presented in Farooqi [33].

(Ramberg–Osgood $M-\theta$ Parameters):

$$M_y = e^{0.507} (g)^{-0.003} (d_b)^{1.130} (p_f)^{0.448} (b_p)^{0.139} (t_p)^{0.095} \times (t_f)^{0.117} (t_w)^{0.134} (h)^{1.136} (F_y)^{0.296} \quad (4)$$

$$\theta_y = e^{-6.266} (g)^{0.555} (d_b)^{0.231} (p_f)^{2.938} (b_p)^{-0.499} (t_p)^{-0.563} \times (t_f)^{-0.080} (t_w)^{-0.485} (h)^{-1.102} (F_y)^{-0.062} \quad (5)$$

$$\xi = e^{16.315} (g)^{0.077} (d_b)^{0.974} (p_f)^{0.946} (b_p)^{-1.009} (t_p)^{-0.478} \times (t_f)^{-0.287} (t_w)^{-0.451} (h)^{0.011} (F_y)^{-1.363} \quad (6)$$

(Three-Parameter Power model $M-\theta$ Parameters):

$$M_u = e^{2.915} (g)^{-0.017} (d_b)^{1.521} (p_f)^{-0.107} (b_p)^{0.070} (t_p)^{0.060} \times (t_f)^{0.064} (t_w)^{-0.009} (h)^{1.085} (F_y)^{0.140} \quad (7)$$

$$\theta_0 = e^{-2.030} (g)^{0.517} (d_b)^{0.164} (p_f)^{1.167} (b_p)^{-0.012} (t_p)^{-1.528} (t_f)^{-0.191} (t_w)^{-0.707} \times (h)^{-1.817} (F_y)^{-0.352} (M_u)^{0.884} (n)^{-0.600} (R_{ki})^{-3.686} (dm/d\theta)^{3.559} \quad (8)$$

$$\zeta = e^{3.370} (g)^{-0.174} (d_b)^{2.013} (p_f)^{-0.277} (b_p)^{0.286} (t_p)^{0.814} (t_f)^{0.275} \times (t_w)^{0.240} (h)^{1.928} (F_y)^{0.640} (M_u)^{-1.759} (R_{ki})^{-1.021} (dm/d\theta)^{1.011}. \quad (9)$$

It should be noted that the variables with powers close to zero or unity can be dropped from Eq. (4) through (9). For example, $(t_w)^{-0.009}$ and $(dm/d\theta)^{1.011}$ can be dropped from Eqs. (7) and (9), respectively. Also, in obtaining Eq. (8) for θ_0 as defined by Eq. (3), the experimentally obtained value of initial stiffness, K_i , by Srouji [8] is based on incrementally loading and unloading the test specimens during the course of experiment. Thus, the unloading slopes of the $M-\theta$ curves are used to indicate the initial connection stiffness. This concept is also supported by Bjorhovde and Brozzetti [34].

Moreover, derivatives of Eqs. (1) and (2) with respect to the connection rotation exist, and they represent the connection's tangential stiffness, K_t . Thus, the initial connection stiffness can be calculated and is bounded when a small value of rotation ($\theta = 10^{-6}$ rad) is substituted in the expression for K_t [35]. For example, Eq. (10) (below) presents the expression for the initial stiffness obtained from Three-Parameter Power model equation.

$$K_i = \frac{M}{\theta [1 - (M/M_u)^n]^{1/n}}. \quad (10)$$

By being able to obtain parameters such as K_i and M_u for a given connection, the mathematical equations presented here can be used in the practical design procedures. For example, the above information can be used to classify a connection based on the choice of either “reference length” or “ultimate strength level” developed by Bjorhovde et al. [18].

Figs. 10–12 show comparisons between typical FEM $M-\theta$ results and the predicted Ramberg–Osgood $M-\theta$ model values obtained by employing Eq. (1) through (3). It can be seen from these figures that the predicted curves give very close correlation with experimental FEM in the elastic region, while it predicts stiffer $M-\theta$ in the post-yield regions.

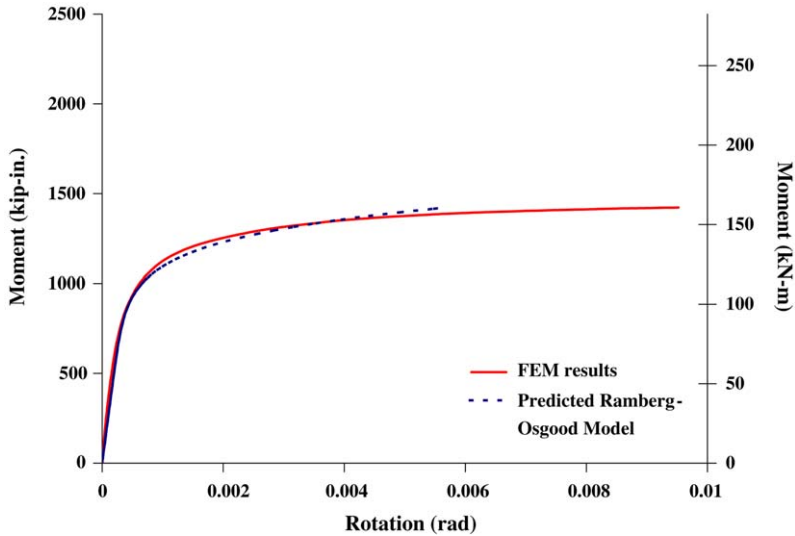


Fig. 10. Comparison of experimental FEM with predicted Ramberg–Osgood model: FEP 2 3/4-3/4-1 3/4-5-1/2-3/8-3/16-24-36.

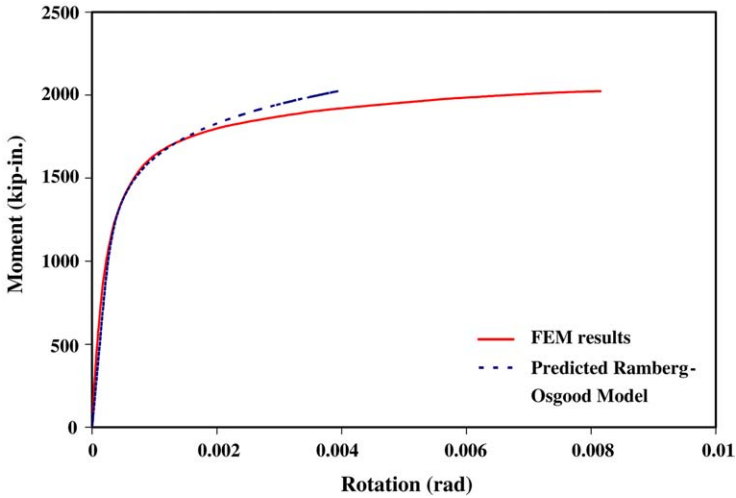


Fig. 11. Comparison of experimental FEM with predicted Ramberg–Osgood model: FEP 2 3/4-1-1 3/4-7-1/2-3/8-3/16-24-36.

Similarly, Figs. 13–15 compare predicted $M-\theta$ obtained from Three-Parameter Power model equation using Eqs. (7)–(9) with those obtained from the FEM analyses. These graphs show excellent correlation over the elastic and inelastic $M-\theta$ regions. Test case designations are as follows: FEP- $g-d_b-p_f-b_p-t_p-t_w-h-F_y$, where FEP stands for flush end-plate connection.

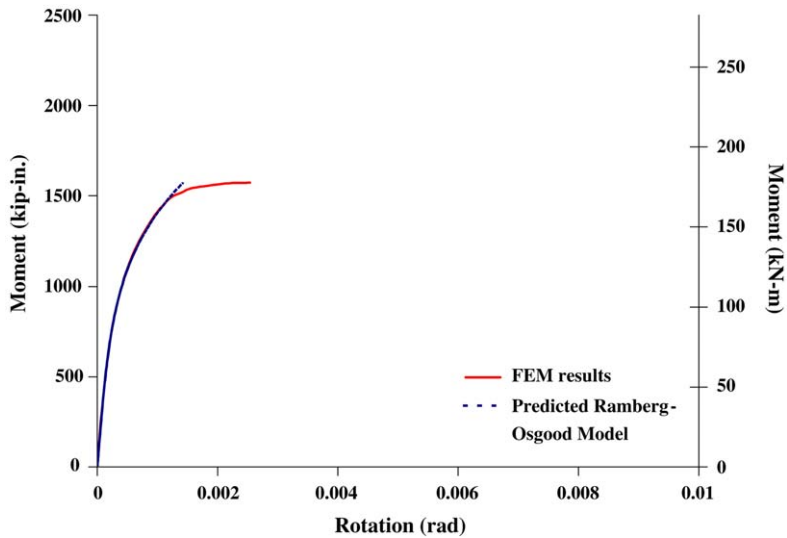


Fig. 12. Comparison of experimental FEM with predicted Ramberg–Osgood model: FEP 2 3/4-3/4-1 1/8-7-1/2-3/8-3/16-24-36.

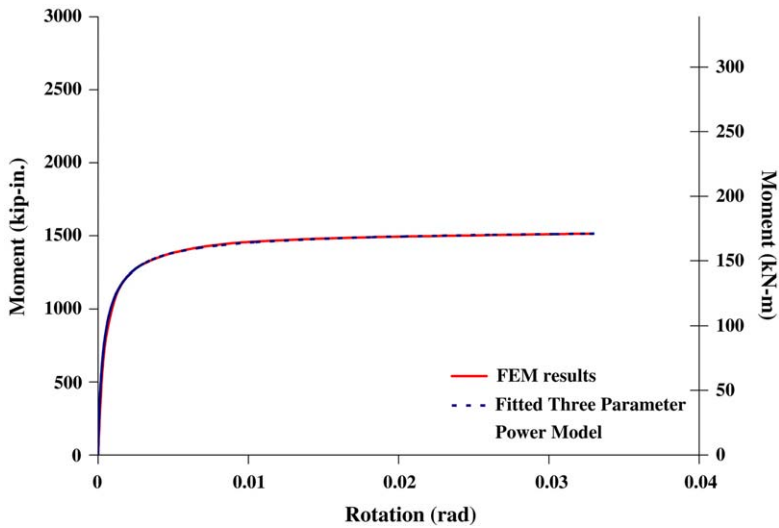


Fig. 13. Comparison of experimental FEM and fitted Three-Parameter Power model: FEP 2 3/4-3/4-2 1/2-7-1/2-3/8-3/16-24-36.

6. Conclusions

A three-dimensional nonlinear finite element (FEM) model was generated by using the FEM software package ANSYS version 6.0 for flush end-plate connections with one row

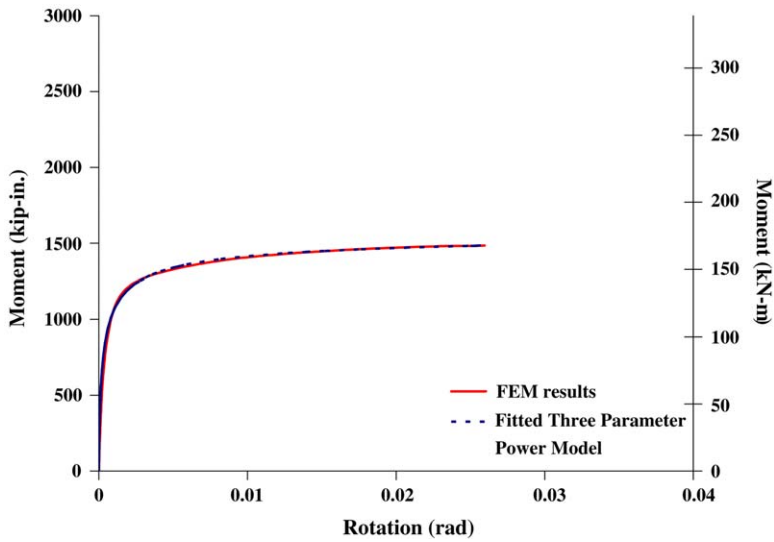


Fig. 14. Comparison of experimental FEM and predicted Three-Parameter Power model: FEP 2 3/4-3/4-1 3/4-7-1/2-3/8-1/10-24-36.

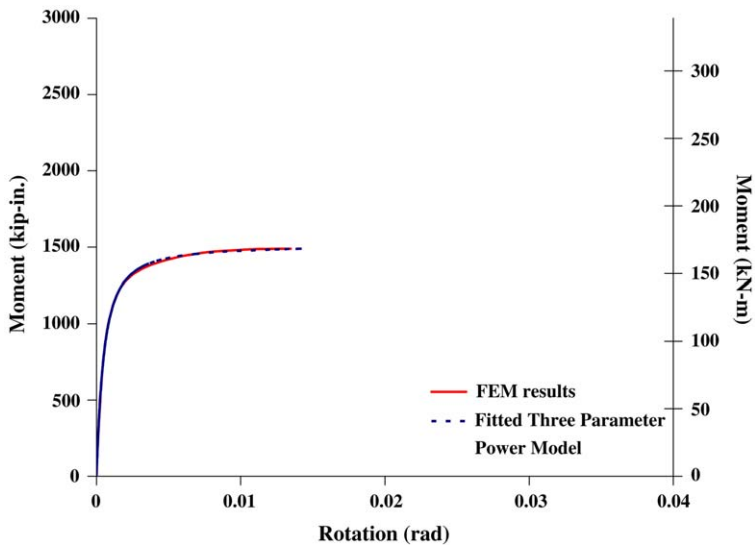


Fig. 15. Comparison of experimental FEM and predicted Three-Parameter Power model: FEP 2 3/4-3/4-1 3/4-7-5/16-3/8-3/16-24-50.

of bolts below the tension flange. Three-dimensional isoparametric 8-noded elements were used to model the end-plate, beam, column, and bolts. The welds were modeled with three-dimensional tetrahedral elements. Nonlinear analyses were adopted to account for material,

geometric, and contact phenomena. ANSYS's bolt pretension element was used to simulate the effects of slip critical bolts with proof load. A bilinear material model was used with initial stiffness, E , and post-yield stiffness, $E_t = 0.1E$. The developed FEM model and its associated nonlinear algorithm were used to obtain the $M-\theta$ behavior of the connections' geometry tested experimentally by Srouji [8].

A test matrix of 34 test cases was developed by varying the flush end-plate's geometric variables within their practical ranges. The FEM model was used to analyze the 34 test cases for $M-\theta$ data, which were curve fitted to Ramberg–Osgood and Three-Parameter Power model equations to obtain defining parameters. Regression equations were developed for the prediction models for flush end-plate connections. It was shown that both models predicted the $M-\theta$ plots closely, with the more accurate model being the Three-Parameter Power model.

References

- [1] Wilson WM, Moore HF. Tests to determine the rigidity of riveted joints in steel structures. Bulletin No. 104. Urban: Engineering Experimentation Station, University of Illinois; 1917.
- [2] Rathbun JC. Elastic properties of riveted connections. Transactions of the ASCE 1936;101:524–63 [Paper No. 1933].
- [3] Bell WG, Chesson E, Munse WH. Static tests on standard riveted and bolted beam-to-column connections. Engineering Experimentation Station, University of Illinois; 1958.
- [4] Douty RT, McGuire W. High strength bolted moment connections. Journal of the Structural Division, ASCE 1965;91(ST2):101–28.
- [5] Sommer WH. Behavior of welded header plate connections. Masters thesis, Ontario (Canada): University of Toronto; 1969.
- [6] Ostrander JR. An experimental investigation of end-plate connections. Master of science thesis. University Saskatchewan; 1970.
- [7] Johnstone ND, Walpole WR. Bolted end-plate beam-to-column connections under earthquake type loading. Research Report 81-7. Christchurch (New Zealand): Department of Civil Engineering, University of Canterbury; 1981.
- [8] Srouji R, Kukreti AR, Murray TM. Strength of two tension bolt flush end-plate connections. Research Report No. FSEL/MBMA 83-03. Norman (OK): Fears Structural Engineering Laboratory, School of Civil Engineering and Environmental Science, University of Oklahoma; 1983.
- [9] Azizinamini A, Radziminski JB. Static and cyclic performance of semi-rigid steel beam-to-column connections. Journal of Structural Engineering, ASCE 1989;115(12):2979–99.
- [10] Frye MJ, Morris GA. Analysis of flexibly connected steel frames. Canadian Journal of Civil Engineering 1975;2.
- [11] Ang KM, Morris GA. Analysis of three-dimensional frames with flexible beam–column connections. Canadian Journal of Civil Engineers 1984;11:245–54.
- [12] Ramberg W, Osgood WR. Description of stress–strain curves by three parameters, Technical Note No. 902. Washington (DC): National Advisory Committee for Aeronautics; 1943.
- [13] Packer JA, Morris LJ. A limit state design method for tension region of bolted beam–column connections. The Structural Engineer 1977;55(10):446–58.
- [14] Zoetemeijer P. Semi-rigid bolted beam-to-column connections with stiffened column flanges and flush-end plates. In: Proceedings of the international conference: joints in structural steelwork: The design and performance of semi-rigid and rigid joints in steel and composite structures and their influence on structural behavior. 1981 p. 2.99–2.118.
- [15] Phillips J, Packer JA. The effect of plate thickness on flush end-plate connections. In: Joints in structural steel work [Proceedings of international conference on joints in steel work]. New York (Toronto): John Wiley and Sons; 1981. p. 6.77–6.92.

- [16] Bijlaard FSK, Zoetemeijer P. Influence of joint characteristics on the structural performance of frames. In: Pavlovic MN, editor. *Steel structures: Recent research advances and their application to design*. London (UK): Elsevier Applied Science Publishers, Ltd; 1986. p. 109–34.
- [17] Bjorhovde R, Brozzetti J, Colson A. *Connections in steel structures: Behavior, strength and design*. London, England: Elsevier Applied Science Publisher; 1988.
- [18] Bjorhovde R, Colson A, Brozzetti J. Classification system for beam-to-column connections. *Journal of Structural Engineering* 1990;116(11):3059–76.
- [19] Barakat M, Chen WF. Practical analysis of semi-rigid frames. *Engineering Journal-American Institute of Steel Construction* 1990;27(2):54–68.
- [20] Xu L, Sherbourne AN, Grierson DE. Optimal cost design of semi-rigid, low-rise industrial frames. *Engineering Journal, AISC* 1995;87–97 (third quarter).
- [21] Yee YL, Melchers RE. Moment–rotation curves for bolted connections. *Journal of Structural Engineering, ASCE* 1986;112(3):615–35.
- [22] Kishi N, Chen WF. Moment–rotation relation of top- and seat-angle connections. *Structural Engineering Report No. CE-STR-86-26*. West Lafayette (IN): School of Civil Engineering, Purdue University; 1987.
- [23] Kishi N, Chen WF. Moment–rotation semi-rigid connections. *Structural Engineering Report No. CE-STR-87-29*, West Lafayette (IN): School of Civil Engineering, Purdue University; 1987.
- [24] Stark JWB, Bijlaard FSK. Structural properties of connections in steel frames. In: *Connections in steel structures: Behaviour, strength, and design*. London (UK): Elsevier Applied Science Publishers; 1988. p. 186–94.
- [25] Krishnamurthy N. Fresh look at bolted end-plate behavior and design. *Engineering Journal, AISC* 1978; 15(2):39–49 [second quarter].
- [26] Ghassemieh M, Kukreti AR, Murray TM. Inelastic finite element analysis of stiffened end-plate moment connections. *Research Report No. FSEL/MBMA 83-02*. Norman (OK): Fears Structural Engineering Laboratory, School of Civil Engineering and Environmental Science, University of Oklahoma; 1983.
- [27] Bahaari MR, Sherbourne AN. Computer modeling of an extended end-plate bolted connection. *Computers and Structures* 1994;52(5):879–93.
- [28] Bahaari MR, Sherbourne AN. Structural behavior of end-plate bolted connections to stiffened columns. *Journal of Structural Engineering, ASCE* 1996;122(8):926–35.
- [29] Summer EA, Mays TW, Murray TM. End-plate moment connections: test results and finite element method validation. In: *Connections in steel structures [The fourth international workshop in steel structures]*. 2000.
- [30] Choi CK, Chung GT. A gap element for three-dimensional elasto-plastic contact problems. *Computers and Structures* 1996;61(6):1155–67.
- [31] Richard RM, Abbott BJ. Versatile elastic–plastic stress–strain formula. *Journal of the Engineering Mechanics Division, ASCE* 1975;101(EM4):511–5.
- [32] Chen WF, Kishi N. Moment–rotation relation of top and seat angle connections, CE-STR-87-4. In: *Proceedings of the international colloquium on bolted and special connections*. 1989.
- [33] Farooqi M. Finite element-based mathematical moment–rotation model for flush end-plate connections. A thesis submitted as partial fulfillment for degree of Master of science. Arlington (TX): Department of Civil and Environmental Engineering, University of Texas at Arlington; 2003.
- [34] Bjorhovde R, Brozzetti J. Data sheet format presentation. In: *Connections in steel structures: Behavior, strength, and design*. London (UK): Elsevier Applied Science Publishers; 1988. p. 380–7.
- [35] Abolmaali A, Kukreti AR, Razavi H. Nonlinear finite element analysis of steel frames with semi-rigid joints. In: *The Proceedings of the Texas section ASCE spring 2002 meeting*. 2002, p. 283–92.